4148 *Macromolecules* **2009**, *42*, 4148–4154
DOI: 10.1021/ma900422n

Macromolecules
ARTICLE

Shear-Induced Ordering of Ferroelectric Crystals in Spin-Coated Thin Poly(vinylidene fluoride-*co*-trifluoroethylene) Films

Hee Joon Jung,[†] Jiyoun Chang,[†] Youn Jung Park,[†] Seok Ju Kang,[†] Bernard Lotz,[‡] June Huh,[†] and Cheolmin Park*,[†]

[†]*Department of Materials Science & Engineering, Yonsei University, Seoul, 120-749 Korea, and* [‡]*Institut Charles Sadron (CNRS-ULP), 6, rue Boussingault, 67083 Strasbourg, France*

Received February 24, 2009; Revised Manuscript Received April 13, 2009

ABSTRACT: We present a robust route for fabricating a thin ferroelectric poly(vinylidene fluoride-*co*-trifluoroethylene) (PVDF-TrFE) film with both molecular and microstructural crystal ordering over the area of 1×1 cm^2. The method is based on the static mechanical shearing of the film under appropriate thermal conditions. The apparatus designed particularly for ultrathin PVDF-TrFE films with thickness of 200 nm or less allowed us to fabricate a thin film with ca. 25 nm thick crystalline lamellae globally ordered perpendicular to the shear direction. Grazing incident X-ray diffraction and polarized near edge X-ray absorption fine structure further revealed the molecular orientation of the crystals with *c* and *a* axes of the PVDF-TrFE crystals preferentially oriented parallel to shear direction and film surface normal, respectively. The shearing of a thin film at 135 °C gave rise to the best crystal orientation directly correlated with approximately 50% enhanced ferroelectric polarization observed in a metal/sheared PVDF-TrFE/metal capacitor.

Introduction

Information storage devices fabricated from ferroelectric polymers such as poly(vinylidene fluoride) (PVDF) and its copolymers with trifluoroethylene (TrFE) have drawn great attention with their potential use for nonvolatile memory technology, one of the most essential technologies for realization of full organic electronic devices.[1−3] Solution-processed thin polymer films are easily sandwiched between two electrodes, leading to a metal/ferroelectric/metal (MFM) capacitor.[3] Permanent dipole moments pointing from fluorine to hydrogen in the ferroelectric state result in a macroscopic polarization with their switching accomplished by rotating the polymer backbone around the chain axis upon a large electric field opposing the polarization.[4,5] Furthermore, for nonvolatile memory with a nondestructive readout capability and a smaller cell size, a memory structure based on the ferroelectric field-effect transistor (FeFET) has been extensively investigated with ferroelectric thin films as gate dielectric.[2,6,7]

Because of the high coercive field of approximately 50 MV/m for PVDF-TrFE, the low operating voltage of less than 10 V simply put a limit to the film thickness, particularly with capacitor architecture. There are two main issues in thin PVDF-TrFE films applicable to memory devices: crystallinity as a function of film thickness and crystal orientation with respect to electric field. Despite the recent promising reports by Naber et al.[8] and Xu et al.[9] with a conducting polymer interlayer inserted between PVDF-TrFE and electrode, the general relationship between layer thickness and remanent polarization (P_r) in spin-coated PVDF-TrFE capacitors shows the abrupt decline of P_r in sub-100 nm PVDF-TrFE films attributed to the decrease in crystallinity in PVDF-TrFE thin films.[10,11] The optimum crystal orientation of the *b* axis parallel to the electric field was abruptly changed to one perpendicular to the electric field either with the decrease in film thickness or upon melting and recrystallization, giving rise to significant reduction of polarization.[12] The ferroelectric polarization also depended on the chemical nature of the electrode controlled by self-assembled monolayers (SAMs) that leads to different orientation of the PVDF-TrFE crystals.[13]

A single crystal-like PVDF-TrFE thin film with the crystal orientation optimized for the electric field would therefore be the most suitable for realization of high-performance ferroelectric polymer memory. The microstructure composed of the characteristic 200 nm long and 40 nm wide crystalline lamellae typically nucleates randomly and grows as a polygranular texture. Several techniques are currently used for inducing long-range order of the microstructure in PVDF-TrFE. They rely on the ability to couple an externally applied field to some molecular or supermolecular feature in the polymer and include crystallographic matching on a surface known as epitaxy,[14,15] localized thermal gradient,[16] directional solvent evaporation,[17] and mechanical fields.[18−20] We have also demonstrated that a thin PVDF-TrFE film is epitaxially oriented in both molecular and microstructure on the friction-transferred highly ordered poly(tetrafluoroethylene) (PTFE) surface.[21] Our method is still limited because it needs an additional interlayer, PTFE, formed on a substrate for epitaxy. It would be optimal if one could find a way in which the global orientation could be achieved on any substrate without an additional layer.

In particular, the mechanically driven forces such as extension and compression have been very effective not only for inducing polymorphic transition to ferroelectric γ or β crystals in PVDF but also for fabricating a single crystal of PVDF-TrFE.[22] The mechanical drawing is a traditional technique to produce β-type ferroelectric crystals by forming the extended all-trans conformation of polymer chains in several micrometers thick PVDF films rarely applicable for the low operating memory.[17,18] Although a recent work by Wang et al.[23] has proposed a method based on the previous pioneering works by Petermann et al.[24] for fabricating ultrathin melt-drawn film with ordered β crystals by melting and recrystallization on the evaporated carbon surface, the film has yet to be employed in device architecture. From the industrial point of view, spin coating is one of the most desirable methods

*Corresponding author. Tel: 02-2123-2833. Fax: 02-312-5375. E-mail: cmpark@yonsei.ac.kr.

 Published on Web 05/14/2009

for uniform film formation and thus provides a great benefit when it is incorporated in fabricating PVDF-TrFE-based devices. To fabricate single crystal-like PVDF-TrFE films spin coated with a thickness of less than 200 nm, we utilized static shearing greatly motivated by the recent work by Register et al.,[25,26] where global microdomain orientation was achieved of thin poly(styrene-*block*-ethylenepropylene) copolymer films by static shearing in on a Si substrate.

In this article, we describe a new way to control both molecular and microstructural orientation in a thin spin-coated PVDF-TrFE film by static shear. A sheared film exhibits monolithic single-crystal-like texture in which approximately 25 nm thick crystalline lamellae are globally oriented perpendicular to the shear direction with *c* and *a* axes of crystals parallel to the shear direction and the film surface normal, respectively. Facile formation of an ordered thin film on a variety of substrates allowed us to fabricate MFM capacitors with the sheared PVDF-TrFE ferroelectric film, which displayed ca. 50% enhanced ferroelectric polarization at the operating voltage of ±20 V arising from the globally ordered molecular and microstructure.

Experimental Section

Thin Film Preparation. A PVDF-TrFE with 27.5 wt % TrFE employed in our study was kindly supplied by MSI Sensor, PA. The melting (T_m) and Curie (T_c) temperatures of the polymer are 150 and 80 °C, respectively. PVDF-TrFE solutions in dimethylformamide (DMF) with the concentration ranging from 1 to 5 wt % were spin coated to form thin polymer films on Aluminum substrates with the spin rate of 3000 rpm for 1 min. Film thickness varied from 50 to 300 nm measured by ellipsometry (Spectroscopic ellipsometer SE MG 1000) and cross-section image with a scanning electron microscope.

Shearing Process. A poly(methylsiloxane) (PDMS) pad with a thickness of approximately 100 μm was placed on the PVDF-TrFE film not only to have uniform mechanical field but also to avoid possible frictional damage of the film during shear. The PDMS/PVDF-TrFE bilayered sample on Al substrate was pressurized with approximately 10^5 Pa by pressure controller and was firmly fixed on the bottom heating plate capable of controlling the temperature up to 250 °C. The heating plate with the sample was moved with the moving velocity controlled by the voltage applied to the DC motor, as shown in both schematic and photograph in Figure 1a. The lateral force was set up to approximately 1 N in our apparatus. The resulting shear stress ($\sim 10^4$ Pa) caused the immediate elastic distortion of the PDMS pad and subsequently gave rise to slow linear displacement arising from viscous shear flow of the PVDF-TrFE film, as illustrated in Figure 1b,c.

The displacement monitored using a micrometer connected to the DC motor is linearly varied with the constant velocity tuned between 0.3 and 1.0 mm/h, depending on the voltage applied. A particular example of the linear displacement of the PDMS pad in our apparatus is shown with the velocity of 1.0 mm/h in Figure 1b. The static shear field was also combined with various thermal treatments of PVDF-TrFE thin films spin coated and covered with a PDMS pad on Al substrate, as depicted in Figure 1d. A PVDF-TrFE film was heated over its melting temperature during 30 min and was subsequently cooled to three different temperatures of 145, 135, and 125 °C at which shear force began to be exerted on the sample with the pressure applied. The PDMS pad we used is 1.0 × 1.0 cm^2 in size in most of cases. All shearing experiments were done within 2 h, and the maximum displacement in our experiment setup is approximately 2 mm in total with the velocity of 1.0 mm/h. Translation velocity after shear stress was measured to be approximately 300 nm s^{-1}, and shear rate became 2 s^{-1} with a 150 nm thick film. The apparent thin-film viscosity calculated in turn was on the

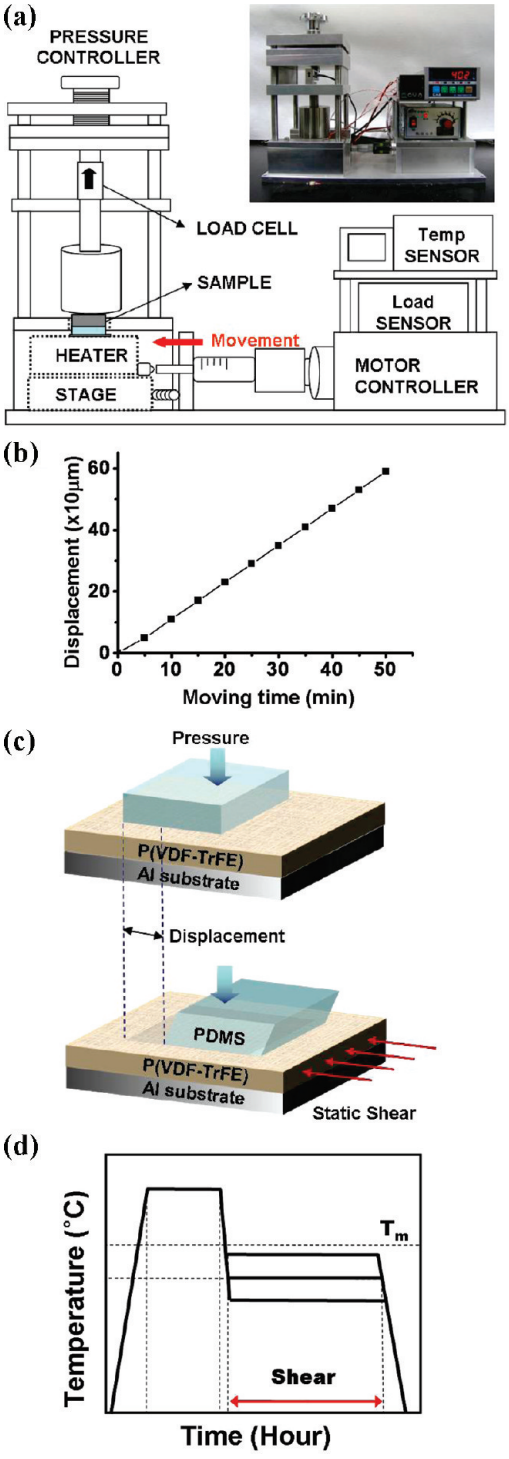

Figure 1. (a) Schematic diagram of the static shear apparatus in which a 100 nm thick PVDF-TrFE thin film fixed and located on a heating stage laterally moves by an electric motor under pressure applied to the sample. An elastomeric PDMS pad in conformal contact on the PVDF-TrFE film is used for uniform shear field on the sample. The inset shows a photograph of the shearing equipment designed in the laboratory. (b) Plot of displacement of a PVDF-TrFE sample as a function of the moving time of motor controller. The sample displacement defined by the distance of a sample during static shear, as illustrated in the schematics of c, is linearly controlled by the motor, giving rise to a static shear field with the constant velocity ranging from 0.1 to 1.0 mm/h. (c) Schematics of PVDF-TrFE/PDMS bilayered sample prior to and under static shear field. (d) Heating profiles of PVDF-TrFE thin films combined with the shearing process. The films are premelted at 180 °C for 30 min and slowly cooled to a temperature below T_m, at which the shear field is applied for 2 h.

order of 10^4 Pa s when possible slip was completely ignored at the interfaces of the polymer layer.

Ferroelectric Polarization Measurement. We prepared metal/ferroelectric/metal capacitors by depositing aluminum top electrodes of 200 μm in diameter on the sheared PVDF-TrFE thin films by thermal evaporation under 10^{-6} mB pressure with a deposition rate of ~0.1 nm/s. Ferroelectric properties were obtained using a virtual ground circuit (Radiant Technologies Precision LC units).

Structure Characterization. The microstructural orientation of sheared PVDF-TrFE thin films was characterized by field emission scanning electron microscope (FESEM) (Jeol 2000) and tapping mode atomic force microscope (AFM) (Nanoscope IV, Digital Instrument). The molecular ordering of the PVDF-TrFE crystals was investigated by 2D grazing-incidence X-ray diffraction (GIXD). The GIXD was performed on the 4C2 beamline at the Pohang Accelerator Laboratory in Korea (incidence angle: ~0.09− 0.15°). The samples were mounted on an X and Y axes goniometer. Monochromatized X-rays (λ = 0.1608 nm) under vacuum and the full range of available incidence angles were used. The scattered beam intensity was recorded with an SCX 4300-165/2 CCD detector (Princeton Instruments). We obtained 2D GIXD patterns in the range $0 < q_z < 2.33$ Å^{-1} and $0 < q_{xy} < 2.33$ Å^{-1}($q = 4\pi \sin\theta/\lambda$, with Z perpendicular and XY parallel to the substrate). We obtained Azimuthal intensity plots of 2D GIXD patterns using FIT 2D software provided by European Synchrotron Radiation Facility. Near edge X-ray absorption fine structure (NEXAFS) experiments were performed on the 4b1 beamline at the Pohang Accelerator Laboratory in Korea. NEXAFS scans were required at the C−K absorption edge. We used p-polarized light to investigate the directional orientation of the crystalline PVDF-TrFE structure by static shear. The sheared samples were mounted with the shear direction aligned either perpendicular or parallel to polarization of the incident light (photon energy, ~270−320 eV) in a vacuum jar (8×10^{-9} torr) and transferred to the analysis chamber where NEXAFS spectra were collected with varying angle of incident light.

Results and Discussion

Static shear field on a few hundred nanometer thick PVDF-TrFE film was applied by the lab-made apparatus shown in Figure 1a. In addition, the displacement of a PDMS pad placed on the PVDF-TrFE film arose from viscous flow of the film during shear, as illustrated in Figure 1c, and varied linearly with time, for example, at the velocity of 1.0 mm/h in Figure 1b. A PVDF-TrFE film was heated over its melting temperature at 180 °C during 30 min and subsequently cooled to three different temperatures of 145, 135, and 125 °C at which shear force began to be exerted on the sample with the pressure applied, as depicted in Figure 1d.

The microstructure of a 150 nm thick PVDF-TrFE film sheared at 135 °C is revealed by both FESEM and AFM, as shown in Figure 2a,b, respectively. The edge-on crystalline lamellae of approximately 25 nm in width are well aligned perpendicular to the shear direction, as indicated by the arrow in Figure 2a. The ordering occurs within 2 h over an area larger than 1 cm^2. Except for some localized mechanical tearing of the film due to nonuniform contact with a PDMS pad, the film indeed shows a global orientation. The sheared regions are almost same in thickness as the nonsheared ones, which implies that the pressure applied during shearing did not play a role in ordering the crystalline domains. In fact, no orientation of PVDF-TrFE lamellae was obtained in a sample that was simply pressed by PDMS without shear. It should also be noted that the pressure we applied was too low to affect the melting and Curie temperature of PVDF-TrFE.[27] The premelting step applied at 180 °C for 30 min turned out to be especially effective for the global

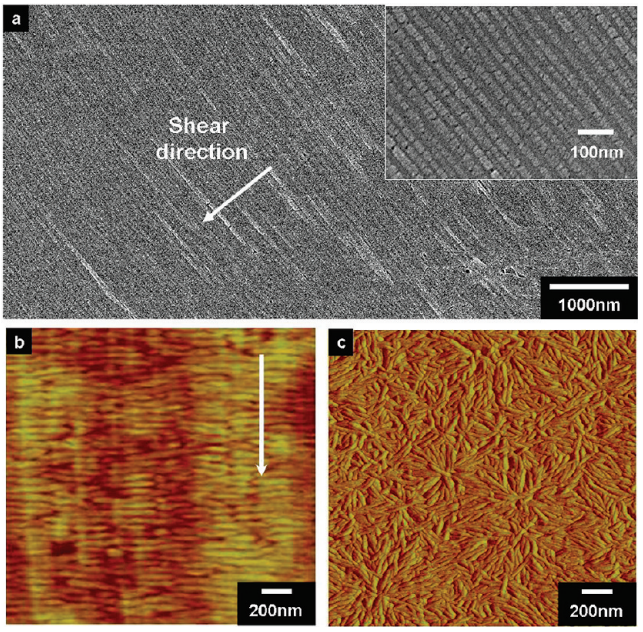

Figure 2. (a) FESEM image of a 150 nm thick PVDF-TrFE film sheared at 135 °C on Al substrate. The semicrystalline lamellae are globally ordered perpendicular to the shear direction, indicated by an arrow over a very large area. The magnified image shown in the inset of a clearly exhibits the ordered edge-on lamellae of approximately 25 nm in width. TM-AFM images in height contrast of (b) a PVDF-TrFE film sheared at 135 °C and (c) a film spin coated and subsequently annealed at 135 °C. The surface topology of the highly ordered crystalline edge-on lamellae is well developed in the sheared sample, whereas the characteristic needlelike crystalline domains are randomly grown in the nonsheared one.

orientation of the crystalline lamellae. A sample spin coated and subsequently sheared at 135 °C without the premelting step still exhibits some ordering of the crystals but much worse than that shown in Figure 2a.

The directional orientation of the crystalline lamellae requires an external field coupled to the polymer crystallization. Two important conditions should be met for the successful ordering. First of all, the external field itself needs to be strong enough to reorient or reorganize the polymer crystals. More importantly, the field should be correlated with the dynamic behavior of the crystalline domains, which is mostly related to both the relaxation time (τ) of polymer chains composing the crystalline domains and the shear rate ($\dot{\gamma}$) applied. The Weissenberg number (W_e), the dimensionless product of a characteristic relaxation time and the shear rate, $W_e = \dot{\gamma}\tau$, and preshear imposed on a sample were both proposed as important factors of flow effects on crystallization.[28] In general, shearing above $W_e = 1$ reduces the density of molecular entanglements, leading to the preferentially ordered crystalline domains. In addition, the larger preshear is imposed, the better alignment of the polymer crystals is obtained within the short period of time. The relaxation time can be estimated to be the time it takes for a molecule to diffuse a distance equal to a crystalline lamellae spacing λ = 40 nm in our case. The relaxation time has $\tau = \lambda^2/D_0$, where D_0 is the polymer diffusion coefficient. The values of D_0 of most of the semicrystalline polymers in melt state lie in the 10^{-17} to 10^{-15} m^2 s^{-1} range,[29] resulting in a W_e value of 3.2 to 320. Although there are some arguments of PVDF-TrFE chain dynamics in the paraelectric phase of whether they behave like disordered-structure fluid or homogeneous fluid,[30] we assumed that the dynamics behaviors of PVDF-TrFE are similar to those of most semicrystalline polymers. On the basis of the calculation, we have found the shear rate from 0.4 to 2 s^{-1} to be appropriate for the orientation. Our results show that the

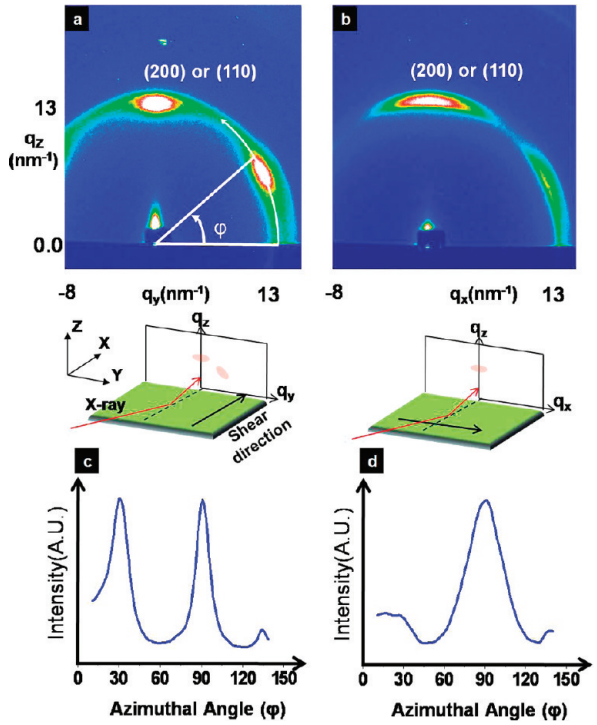

Figure 3. 2D GIDX patterns for a PVDF-TrFE thin film sheared at 135 °C with the incident X-ray beam parallel to the surface normal of the (a) *YZ* and (b) *XZ* planes. When the X-ray beam is parallel to the shear direction, two strong reflections are observed near 13.5 nm^{-1} on both the meridian and 60° away from the meridian in a. However, much stronger meridian reflection is detected with a minor reflection 60° away from the meridian when the incident beam is perpendicular to *XZ* plane in b. The schematics below a and b depict the sample geometry with respect to the grazing incident X-ray beam. Equatorial azimuthal intensity profiles of a and b are shown in (c) and (d), respectively.

orientation of PVDF-TrFE crystals was not significantly affected by the range of the shear rate we employed. It should be also noted that the preshear of our PVDF-TrFE films larger than approximately 1000 seems to be especially helpful for inducing the orientation of the crystals, even with the relatively low W_e values.

The surface morphology of the sheared PVDF-TrFE thin film was compared with that of nonsheared film, as shown in Figure 2b,c, respectively. Again, the well-ordered crystalline lamellae are apparent, aligned perpendicular to the shear direction, whereas the characteristic needlelike lamellae appear to be randomly oriented after spin coating, followed by heat treatment at 135 °C. The coating of thin layer of Pt in SEM for electron beam contrast in the inset of Figure 2a makes the morphology of the ordered sample slightly different from that by AFM.

Molecular orientation of the globally ordered PVDF-TrFE crystalline lamellae was investigated in the 150 nm thick films with GIXD. We defined the flow direction to correspond to *X*, the neutral direction to *Y*, and the through thickness direction to *Z*, as schematically depicted in Figure 3a. The 2D GIXD pattern with the incident X-ray directed along the normal to the *YZ* plane and along the shear direction (*X* axis) clearly exhibits two strong reflections at 13.5 nm^{-1} (i.e., ~4.6 Å) on the "meridian" of the diffraction pattern and some 60° away from the meridian, as shown in Figure 3a. The PVDF-TrFE crystal phase has an orthorhombic lattice that is characterized by a $\sqrt{3}/2$ ratio of its *a* and *b* axes and in turn results in nearly equal (200) and (110) spacings; moreover, these reflections are 60° from one another in an *hk*0 diffraction pattern. As a consequence, it is difficult to index the meridional and off-meridional reflections unambiguously. The diffraction, however, clearly implies that the *ab* plane of the PVDF-TrFE crystals is perpendicular to the X-ray direction; in other words, the *c* axis of the crystals is dominantly parallel to the shear direction. The equatorial azimuthal intensity distribution profile in Figure 3c shows the two reflections separated by 60°, which is indicative of a sixfold hexagonal structure.

A 2D GIXD pattern with the incident beam perpendicular to *XZ* plane supports our argument, as shown in Figure 3b. In this case, the X-ray beam is perpendicular to the shear direction. We observed a strong reflection at the meridian with a much weaker reflection 60° from the meridian. There are two possible scenarios on the basis of Figure 3a,b. When we assume that the meridian reflection in Figure 3a is from (200) of *hk0* reflections corresponding to the *a***b** section of the reciprocal lattice of PVDF-TrFE, the meridian reflection in Figure 3b also corresponds to (200), which is one of the *h0l* reflections arising from the *a***c** section of the reciprocal lattice. The off-meridian (110) reflection appearing in Figure 3a is therefore supposed to be completely suppressed in the case of single-crystal-like texture in which the *bc* plane of the crystals is on contact with the substrate with the *a* axis parallel to the surface normal. In our sheared sample, it should be noted that very weak off-meridian reflection still exists 60° from the meridian because of some misorientation of the crystals, although its intensity is much weaker than that of the (200) reflection, as shown in azimuthal intensity profile of Figure 3d.

In the other case, the (110) reflection is assumed to be located on the meridian in Figure 3a. The meridian reflection in Figure 3b thus corresponds to the (110) reflection with very weak (200) off-meridian reflection. In either case, the shearing applied indeed allows us to produce a PVDF-TrFE thin film with nearly single-crystal-like texture over a large area. It is important to note that the fwhm of the meridian reflection (~11°) in Figure 3c is smaller than that (~30.5°) in Figure 3d, implying the better orientation along the shear direction mainly due to the weaker structural correlation along the neutral direction (*Y* axis) than the shear direction (*X* axis). In fact, the crystalline PVDF-TrFE lamellae aligned perpendicular to the shear direction (*Y* axis) tend to orient with the slight fluctuation, as shown in Figure 2a,c.

To resolve the crystal orientation further, in particular, the orientation of the *a* and *b* axes in a sheared film, we performed a polarized NEXAFS, which provided us the incident-beam-dependent photoemission of the characteristic bonds in PVDF-TrFE chains. As shown in Figure 4e, the polar angle, θ, is defined as the angle between the electric field vector of the light and the sample normal. The azimuthal angle, φ, is defined as the angle between the plane of incidence and the shearing direction. First of all, at $\theta = 90°$, the NEXFAS spectra were obtained at the azimuthal angles of 90 and 0°, as shown in Figure 4a,b, respectively. On the basis of the fact that excitation peaks of σ*(C−F) and σ*(C−C) correspond to 292 and 294 eV, respectively,[31] one can easily notice that the baseline-normalized relative intensity of σ*(C−F) excitation was significantly reduced, even lower than that of σ*(C−C) excitation when φ was changed from 90 to 0°. These results clearly indicate that C−C bonds, that is, the backbone of PVDF-TrFE (the direction of *c* axis), were aligned parallel to the shearing direction, which is consistent with the GIXD results.

The orientation of the *b* and *a* axes of sheared PVDF-TrFE with *c* axis parallel to the shear direction was further revealed by NEXAFS spectra obtained with different θ angles at each φ, as shown Figure 4c,d. For a PVDF-TrFE crystal with its *c* axis parallel to the substrate, C−C bonds are supposed to lie on the substrate when the *a* axis is parallel to the surface normal, as illustrated in the molecular schematic of Figure 6a. In the case of the *b* axis parallel to the surface normal, the chains are rotated to 90° along the chain axis from the previous orientation, resulting in C−C bonds with some angle to the surface. When the polar

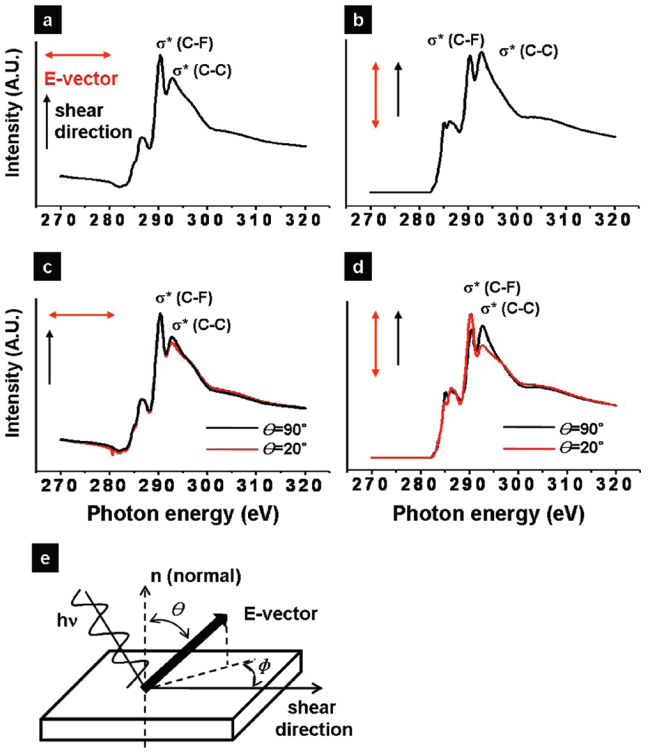

Figure 4. NEXAFS spectra of a sheared PVDf-TrFE thin film collected at (a) $\varphi = 90°$, $\theta = 90°$ and (b) $\varphi = 0°$, $\theta = 90°$. NEXAFS spectra of the film obtained (c) at the polar angle, θ,of both 90 and 20° at $\varphi = 90°$ and (d) at the polar angle, θ, of both 90 and 20° at $\varphi = 0°$. (e) Schematic of NEXAFS geometry with polar angle (θ) defined as the angle between the electric field vector of the light and the sample normal, azimuthal angle (φ), and the electric field vector (**E**) of incident light. φ is set at zero when the plane of incidence is parallel to the shearing direction indicated in the schematic.

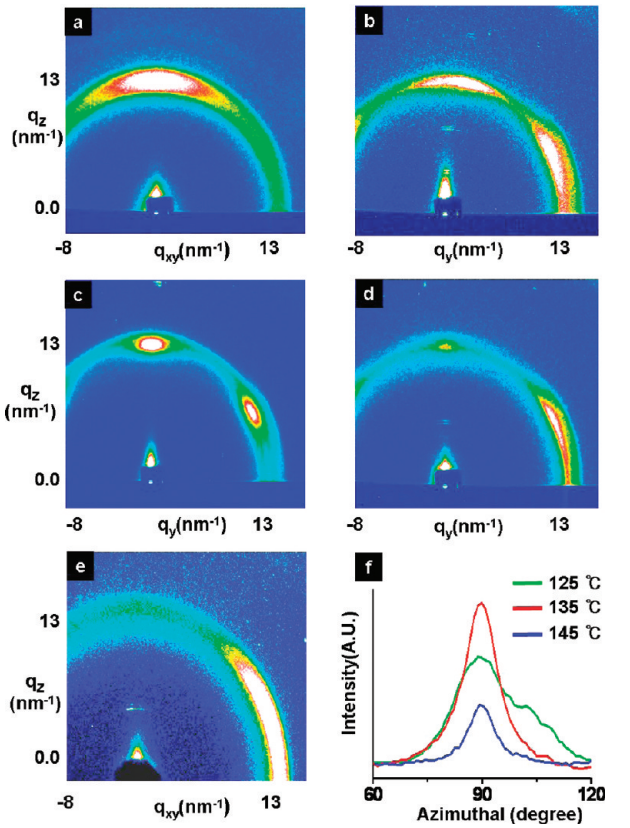

Figure 5. 2D GIDX patterns for PVDF-TrFE thin films spin coated and subsequently annealed at (a) 135 and (e) 200 °C without shear and for PVDF-TrFE films sheared at (b) 125, (c) 135, and (d) 145 °C for 2 h with the incident X-ray beam parallel to the surface normal of *YZ*, that is, the shear direction. The azimuthal intensity profiles of the meridian reflections of b, c, and d represented in (f) clearly indicate that the shearing at 135 °C results in the best molecular orientation of the crystalline lamellae with the most intensified meridian reflection.

angle, θ, was changed from 90 to 20° at $\varphi = 90°$, the intensity of σ^*(C−C) resonance slightly decreased, as shown in Figure 4c. However, the change of the polar angle from 90 to 20° at $\varphi = 0°$ gave rise to the intensity reverse between σ^*(C−C) and σ^*(C−F) excitation, as clearly shown in Figure 4d. These results suggest that C−C bonds lie parallel to the substrate with the *a* axis of the PVDF-TrFE crystals aligned perpendicular to the substrate. For instance, if the C−C bonds were oriented with the angle to the substrate in the case of the *b* axis perpendicular to the substrate, then the relative intensity of σ^*(C−C) to that of σ^*(C−F) would increase in Figure 4c because the C−C bonds are more parallel to the electric vector, and thus the contribution of the C−C bond resonance becomes greater at 20° polar angle. Figure 4d further confirms the *a* axis orientation parallel to the surface normal in which the minimal contribution of σ^*(C−C) due to the large mismatch between C−C bonds and the electric vector of incident light resulted in the intensity reverse of σ^*(C−C) at the polar angle of 20°. Both GIXD and NEXAFS data clearly evidence that the static shearing we employed successfully fabricates a highly ordered PVDF-TrFE film with *c* and *a* axes of the crystals aligned parallel to the shear direction and to surface normal, respectively.

The degree of ordering of the crystalline PVDF-TrFE thin films depends on the temperature at which the shear was applied after the complete melting of a thin film. First of all, a sample spin coated and subsequently annealed at 135 °C for 2 h in Figure 5a exhibits a broadly arced meridian reflection that corresponds to the (110) reflection rotating around the *Z* axis, as we previously investigated in our recent work.[12] In this case, the chain *c* axis dominantly lies parallel to the substrate with the random registry on the *XY* plane, which results in needlelike crystalline lamellae randomly oriented on the substrate very similar to the morphology in Figure 2c. Thin PVDF-TrFE films that were premelted at 180 °C and slowly cooled down below T_m and sheared at 125, 135, and 145 °C for 2 h clearly displayed better molecular orientation in GIXD than that shown in Figure 5a with both meridian and off-meridian reflections with the X-ray beam parallel to the shear direction, as shown in Figure 5b−d, respectively. The alignment of the crystals obviously arose from the crystallization under strain. The best orientation was obtained with the shearing at 135 °C, as clearly indicated by the azimuthal intensity profiles of the meridian reflections in Figure 5f. The intensity of the reflection of the sample sheared at 135 °C is much greater than that of any other samples in the GIXD patterns collected with the same exposure time of 10 s, attributed to more highly ordered crystals by shear (Table 1). The fwhm values for the films sheared at 125 and 135 °C also confirmed the better orientation, as shown in Table 1.

The shearing at the lower temperature (125 °C) may involve a larger number of nuclei subsequently growing into crystalline lamellae during shear than that at the higher temperature (135 °C). A final microstructure arising from shear has relatively short and narrow crystalline lamellae connected and aligned perpendicular to the shear direction with each other with numerous crystalline interlamellae defects at the junctions of two lamellae (data not shown) giving rise to more scattered reflections, as shown in Figure 5b. The increase in shearing temperature was effective in our system for orienting the crystalline lamellae as close as T_m. The results of a sample sheared at 135 °C support our argument in Figure 4c.

Table 1. Crystalline and Capacitor Characteristics of the PVDF-TrFE Films Either Annealed or Sheared at Different Temperatures

	meridian reflections				
samples[a]	fwhm	I_{max} at T/I_{max} at 135 °C	crystallinity (%)[b]	remanent polarization (μC/cm^2)	coercive voltage (V)
annealed at 135 °C	NA	NA	63.45	4.32	12.1
sheared at 125 °C	23	0.76	58.94	4.98	7.29
sheared at 135 °C	11.2	1	66.23	6.84	8.74
sheared at 145 °C	NA	0.39	55.17	4.49	8.37

[a] Samples were all premelted at 180 °C for 30 min before treatment. [b] Calculated by construction of crystallinity from the discrimination between the amorphous hump and the crystalline regions in GIXD data.

Further increase in the shearing temperature at 145 °C, however, gave rise to the significant intensity reduction of the meridian reflection at the same time with the enhanced intensity of the off-meridian reflection, as shown in both Figure 5d and Table 1. The dominance of the scattering at off-meridian regions in Figure 5d is partially attributed to the crystals with their *c* axis oriented perpendicular to the surface upon melting and recrystallization of PVDF-TrFE, as reported in our previous work.[12] The characteristic *c*-axis orientation parallel to the surface normal during melting and recrystallization was evidenced by the presence of a strong reflection on the equator in the GIXD pattern that was very similar to one observed in a sample simply melted and recrystallized without shear field in our shear apparatus, as shown in Figure 5e. The tendency of the crystal orientation with the *c* axis perpendicular to the surface during recrystallization was completely forbidden by the directional shear field at the shear temperature sufficiently lower than T_m, as confirmed in Figure 5b,c. When the shear temperature is close to T_m (~145 °C), some of the PVDF-TrFE film may be still in the molten state under shear and recrystallized independently with some amount of crystals aligned with the perpendicular *c* axis to surface. A typical microstructure of a sample sheared at 145 °C exhibits the mixture of the edge-on crystalline lamellae aligned to the shear direction and the in-plane lamellae resulting from the perpendicular *c*-axis orientation.[12] It is also noteworthy that the degrees of crystallization of the sheared samples at different temperatures, calculated from the GIXD results, are all very similar (~60%), which is consistent with our previous results.[12,21]

The formation of a uniformly sheared 150 nm thick film with the global orientation of crystalline PVDF-TrFE lamellae schematically illustrated in Figure 6a allows us to fabricate arrays of metal/sheared PVDF-TrFE/metal capacitors. A capacitor with a top electrode of approximately 200 μm in diameter was easily produced without dielectric breakage of the film over 100 MV/m. Figure 6b shows the ferroelectric polarization hysteresis loops of PVDF-TrFE thin films sheared at 125, 135, and 145 °C. Consistent with the scattering results of Figure 5b−d, a sample sheared at 135 °C exhibits the largest remanent polarization (P_r) of approximately 6.9 μC/cm^2 with the coercive voltage (V_c) of 8.7 V. The P_r value of 4.98 μC/cm^2 was observed at shear temperature of 125 °C. Compared with a controlled sample premelted and subsequently annealed at 135 °C in our shear apparatus, the sheared sample at 135 °C represents the higher P_r with the lower V_c (Table 1). The presence of the in-plane crystalline lamellae, ineffective for ferroelectric polarization, at a sample sheared at 145 °C results in the lowest P_r (~4.5 μC/cm^2) among three samples. The ferroelectric properties of PVDF-TrFE films are summarized in Table 1.

In fact, the molecular orientation of the crystalline PVDF-TrFE lamellae obtained by static shear is almost same as that resulting from the epitaxy of PVDF-TrFE on a PTFE substrate we have recently reported[21] and is not beneficial for effective ferroelectric polarization because the polar *b* axis is perpendicular to the electric field applied parallel to the surface

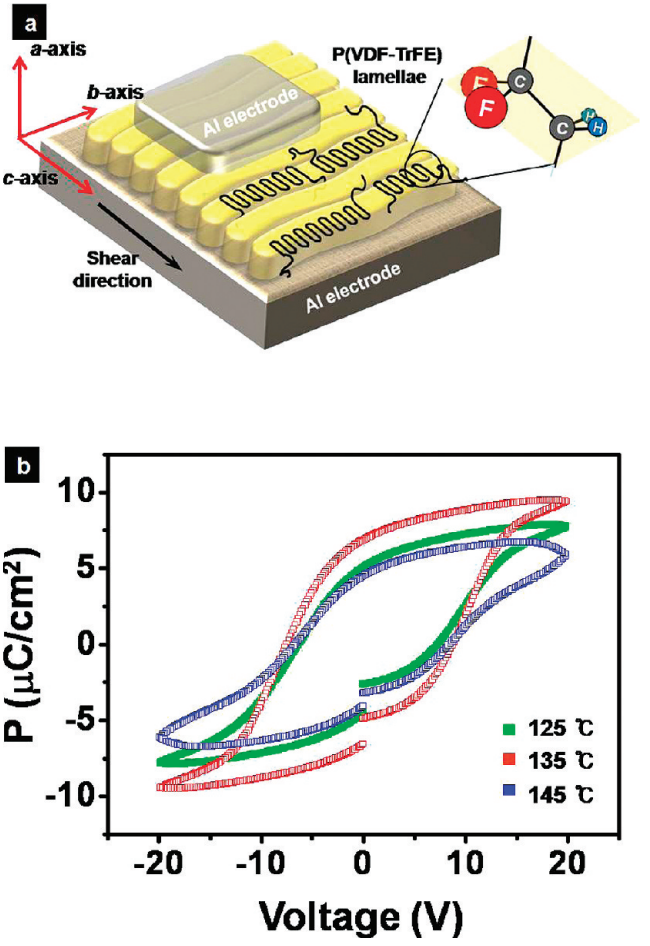

Figure 6. (a) Schematic illustration of a thin PVDF-TrFE film globally ordered by static shear. The crystals are oriented with their *c* and *a* axes parallel to the shear direction and surface normal, respectively. The oriented PVDF monomeric unit is only shown for convenience. (b) Polarization, *P*, versus applied voltage, *E*, hysteresis loops of Al/150 nm-PVDF-TrFE/Al capacitors with ferroelectric PVDF-TrFE films sheared at 125, 135, and 145 °C. The largest remanent polarization of approximately 6.9 μC/cm^2 was obtained with the film sheared at 135 °C arising from the best molecular orientation observed in Figure 5.

normal of the film, as shown in the schematic of Figure 6a. The pseudohexagonal symmetry of crystal structure of PVDF-TrFE, however, allows the orientation shown in Figure 6a to be easily transformed into one with the H−F dipole aligned parallel to the surface normal with a 30° off-angle by rotating the H−F dipole under an electric field. Our previous work demonstrated that the rotation of the dipole required only a slightly higher electric field at the beginning, leading to a final remanent polarization that is very similar to that obtained from a sample with the crystal structure not necessary for the rotation.[12] The maximum polarization that can be obtained with the transformed crystal orientation, similar to that shown in Figure 6b of our previous

publication,[21] is 87% of the ideal polarization of PVDF-TrFE crystals whose *b* axis is completely parallel to the electric field. Further detailed properties of a memory device are under investigation including data retention and fatigue.

Conclusions

We employed static shear for controlling both molecular and microstructural orientation of semicrystalline and ferroelectric PVDF-TrFE thin films. The apparatus capable of shearing 100 nm thick polymer films enabled us to fabricate a globally ordered PVDF-TrFE thin film over an area larger than 1 cm^2. An ordered film formed within 2 h had a chain axis and *c* axis dominantly aligned along the shear direction with the crystalline lamellae unidirectionally oriented perpendicular to the shear. In addition, both GIXD and NEXAFS data clearly evidenced the fact that the *a* axis of the crystals was aligned parallel to the surface normal with the *b* axis on the substrate. The best orientation was obtained in a 150 nm thick film sheared at 135 °C and gave rise to a higher remanent polarization of approximately 6.9 $\mu C/cm^2$ than that from a film simply annealed at 135 °C because of both the effective crystal orientation for polarization switching and the reduced microstructural defects.

Acknowledgment. This project was supported by DAPA and ADD, the National Research Program for the 0.1 Terabit Non-Volatile Memory Development, Samsung Electronics Co., Ltd. and "SYSTEM2010" project sponsored by Korea Commerce, Industry, and Energy. The X-ray experiments at PAL (4C2 beamline), Korea, were supported by MOST and POSCO, Korea. We also thank ESRF for providing a FIT 2D software. This work was supported by the Korea Science and Engineering Foundation (KOSEF) grant funded by the Korea government (MOST) (no. R11-2007-050-03001-0).

References and Notes

(1) Ducharme, S.; Reece, T. J.; Othon, C. M.; Rannow, R. K. *IEEE Trans. Device Mater. Reliab.* **2000**, *5*, 720.
(2) Naber, R. C. G.; Tanase, C.; Blom, P. W. M.; Gelinck, G. H.; Marsman, A. W.; Touwslager, F. J.; Setayesh, S.; de Leeuw, D. M. *Nat. Mater.* **2005**, *4*, 243.
(3) Fujisaki, S.; Ishiwara, H.; Fujisaki, Y. *Appl. Phys. Lett.* **2007**, *90*, 162902.
(4) Bune, V.; Fridkin, V. M.; Ducharme, S.; Blinov, L. M.; Palto, S. P.; Sorokin, A. V.; Yudin, S. G.; Zlatkin, A. *Nature* **1998**, *391*, 874.
(5) Lovinger, A. J. *Science* **1983**, *220*, 1115.
(6) Naber, R. C. G.; de Boer, B.; Blom, P. W. M.; de Leeuw, D. M. *Appl. Phys. Lett.* **2005**, *87*, 203509.
(7) Nguyen, C. A.; Mhaisalkar, S. G.; Ma, J.; Lee, P. S. *Org. Electron.* **2008**, *9*, 1087.
(8) Naber, R. C. G.; Blom, P. W. M.; Marsman, A. W.; de Leeuw, D. M. *Appl. Phys. Lett.* **2004**, *85*, 2032.
(9) Xu, H.; Zhong, J.; Liu, X.; Chen, J.; Shen, D. *Appl. Phys. Lett.* **2007**, *90*, 092903.
(10) Zhang, Q. M.; Xu, H. S.; Fang, F.; Chang, Z.-Y.; Xia, F.; You, H. *J. Appl. Phys.* **2001**, *89*, 2613.
(11) Xia, F.; Xu, H. S.; Fang, F.; Razavi, B.; Chang, Z.-Y.; Lu, Y.; Xu, B.; Zhang, Q. M. *Appl. Phys. Lett.* **2001**, *78*, 1122.
(12) Park, Y. J.; Kang, S. J.; Kim, K. J.; Lee, H. S.; Lee, M. S.; Chung, U.-I.; Park, I. J.; Park, C. *Appl. Phys. Lett.* **2006**, *88*, 242908.
(13) Park, Y. J.; Kang, S. J.; Park, C.; Lotz, B.; Thierry, A.; Kim, K. J.; Huh, J. *Macromolecules* **2008**, *41*, 109.
(14) Noda, K.; Ishida, K.; Horiuchi, T.; Matsushige, K.; Kubono, A. *J. Appl. Phys.* **1999**, *86*, 3688.
(15) Krüger, J. K.; Heydt, B.; Fischer, C.; Baller, J.; Jiménez, R.; Bohn, K.-P.; Servet, B.; Galtier, P.; Pavel, M.; Ploss, B.; Beghi, M.; Bottani, C. *Phys. Rev. B* **1997**, *55*, 3497.
(16) Kimura, K.; Kobayashi, K.; Yamada, H.; Matsushige, K. *Langmuir.* **2007**, *23*, 4740.
(17) Kang, S. J.; Park, Y. J.; Sung, J.; Jo, P. S.; Park, C.; Kim, K. J.; Cho, B. O. *Appl. Phys. Lett.* **2008**, *92*, 012921.
(18) Yang, D. C.; Thomas, E. L. *J. Mater. Sci.* **1984**, *3*, 929.
(19) Yang, D. C.; Thomas, E. L. *J. Mater. Sci. Lett.* **1987**, *6*, 593.
(20) Kaufmann, W.; Petermann, J.; Reynolds, N.; Thomas, E. L.; Hsu, S. L. *Polymer* **1989**, *30*, 2147.
(21) Park, Y. J.; Kang, S. J.; Lotz, B.; Brinkmann, M.; Thierry, A.; Kim, K. J.; Park, C. *Macromolecules* **2008**, *41*, 8648.
(22) Matsushige, K.; Nagata, K.; Imada, S.; Takemura, T. *Polymer* **1980**, *21*, 1391.
(23) Wang, J.; Li, H.; Liu, J.; Duan, Y.; Jiang, S.; Yan, S. *J. Am. Chem. Soc.* **2003**, *125*, 1496.
(24) Petermann, J.; Gohil, R. M. *J. Mater. Sci.* **1979**, *14*, 2260.
(25) Angelescu, D. E.; Waller, J. H.; Adamson, D. H.; Deshpande, P.; Chou, S. Y.; Register, R. A.; Chaikin, P. M. *Adv. Mater.* **2004**, *16*, 1736.
(26) Angelescu, D. E.; Waller, J. H.; Register, R. A.; Chaikin, P. M. *Adv. Mater.* **2005**, *17*, 1878.
(27) Hikosaka, M.; Sakurai, K.; Ohigashi, H.; Koizumi, T. Jpn. *J. Appl. Phys.* **1993**, *32*, 2029.
(28) Elmoumni, A.; Winter, H. H. *Rheol. Acta* **2006**, *45*, 793.
(29) Gell, C. B.; Greassley, W. W.; Fetters, L. J. *J. Polym. Sci., Part B: Polym. Phys.* **1997**, *35*, 1933.
(30) Bellet-Amalric, E.; Legrand, J. F. *Eur. Phys. J. B* **1998**, *3*, 225.
(31) Okudaira, K. K.; Kobayashi, E.; Mase, K.; Kera, S.; Ueno, N. *Surf. Rev. Lett.* **2006**, *13*, 259.